Chemical Engineering Journal Advances 25 (2026) 101007

Contents lists available at ScienceDirect

Chemical Engineering Journal Advances

journal homepage: www.sciencedirect.com/journal/chemical-engineering-journal-advances

Structure-property relationship of phosphonium-based polymerized ionic liquids as anion conducting membranes

Enrica Fontananova [a,*], Francesco Galiano [a], Raffaella Mancuso [b], Daria Talarico [a], Gianluca Di Profio [a], Lorenzo Guazzelli [c], Christian S. Pomelli [c], Mario Ferraro [d,e], Raffaele Filosa [d,e], Vincenzo Formoso [d,e], Raffaele G. Agostino [d,e], Bartolo Gabriele [b,*], Alberto Figoli [a]

[a] Institute on Membrane Technology-National Research Council (ITM-CNR), Via P. Bucci 17/C, 87036, Rende (CS), Italy
[b] Laboratory of Industrial and Synthetic Organic Chemistry (LISOC), Department of Chemistry and Chemical Technologies, University of Calabria, Via Pietro Bucci 12/C, 87036, Arcavacata di Rende (CS), Italy
[c] Department of Pharmacy, University of Pisa, Via Bonanno 33, 56126, Pisa, Italy
[d] Department of Physics and STAR Research Infrastructure, University of Calabria, via Tito Flavio, 87036, Rende(CS), Italy
[e] Institute of Nanotechnology-National Research Council (NANOTEC-CNR), Via Pietro Bucci, Rende, (CS), 87036, Italy

ARTICLE INFO

Keywords:
Anion conducting membrane
Electrochemical properties
Energy
structural properties
Polymerized ionic liquid

ABSTRACT

Membrane technology in sustainable energy conversion and storage requires the development of tailored membranes able to conjugate high performance (ionic conductivity, perm-selectivity and durability) with acceptable costs and sustainability in their production. In this perspective, polymerizable ionic liquids (PILs) are conductive materials suitable to make high-performing and green ion-conductive membranes combining the unique properties of the ionic liquids, with the advantages of a macromolecular crosslinked polymer. This work presents a deep investigation of the structure-property relationship of phosphonium-based PILs as a functional material for anion-conducting membranes produced by casting and successive photopolymerization (almost solvent-free conditions). The PIL-based membranes prepared were dense, flexible, and completely stable after prolonged contact with water, saline and alkaline solutions. The crosslinking reaction avoided the dissolution of the membrane in water. However, mechanical test highlighted the role of water uptake on mechanical properties of the membranes. Moreover, it was also validated the possibility to blend different PILs in order to combine in synergic way the specific advantages of each component. Electrochemical impedance spectroscopy and membrane potential measurements pointed out a trade-off relationship between the ionic conductivity and perm-selectivity. Moreover, Small Angle X-ray Scattering and differential scanning calorimetry findings shed light on the role of the chemical nature of the PIL on membrane microstructure and transport properties. The main outcome of this research is the possibility to balance the low ionic resistance transport through the charged PILs, with a good stability, tailoring the chemistry of these advanced functional materials.

1. Introduction

During the last decades, ion exchange membranes (IEMs) have shown a wide potential in a plethora of membrane-based applications, such as desalination, chemical synthesis, energy conversion, and storage. The reasons behind their success can be mainly attributed to the high efficiency, low environmental impact, and modest electrical energy consumption of the processes related to their application [1].

IEMs are generally made up of polymeric backbones with charged functional groups. Depending on the type of ionic groups contained in the membrane matrix, they can be classified into cation exchange membranes (CEMs), characterized by fixed negative charged groups and exchangeable cations, and anion exchange membranes (AEMs), characterized by fixed positive charged groups and exchangeable anions. An ideal IEM should fulfill a series of requirements, such as high perm-selectivity (namely, the capability to be selectively permeable to counter-ions), high ionic conductivity, and high chemical, thermal, and mechanical stability [2]. However, the preparation of a membrane able

* Corresponding authors.
E-mail addresses: enrica.fontananova@cnr.it (E. Fontananova), bartolo.gabriele@unical.it (B. Gabriele).

https://doi.org/10.1016/j.ceja.2025.101007

Available online 25 December 2025

to satisfy all the above characteristics is not trivial and still to date quite challenging. In this framework, extensive research has been devoted to exploring new materials and novel synthetic strategies for designing and developing IEMs with desired properties and performance [3]. The standard method for producing AEMs, one of the two types of membranes used in electrochemical technologies, is usually based on chloromethylation of an aromatic polymer, such as polysulfone or polystyrene, and quaternization of a benzyl chloride moiety with a tertiary amine to form a cationic quaternary ammonium group bonded to an aromatic ring through a benzyl bond [4]. Polyvinyl alcohol (PVA) [5], poly (2,6-dimethyl-1,4 phenylene oxide) (PPO) [6] and other poly (aromatic ethers) (PAE) [7] are other typical ionomers used for the fabrication of AEMs, while quaternary ammonium [8], imidazolium [9] and pyridinium [10] groups are the most employed cations moieties attached to the ionomer backbone. However, the limited chemical stability in a basic environment, the reduction of perm-selectivity over time, and the simultaneous increase in resistance to counter-ions transport in the presence of multivalent ions are still open challenges in the field of AEMs for electrochemical systems [11].

In recent years, ionic liquids (ILs), which display unique physicochemical properties, have started to be used as novel materials for the preparation of membranes, mainly in CO_2 separation [12–15]. ILs are molten salts below 100°C composed of organic ions that possess high ionic conductivity, high chemical and thermal stability, non-flammability, with potential application in electrochemical processes [16]. Moreover, they are also considered as sustainable solvents with highly tailorable properties, which make them versatile platforms for different applications [17,18].

In most of the works reported in literature, the incorporation of ILs into polymer matrix mainly occurs through their addition directly into the casting solution or by their impregnation into the polymer membrane matrix [19]. For example, Hernández-Fernández et al [20]. prepared a series of supported ionic liquid membranes (SILMs) by imbibing the ionic liquid into a porous Nylon membrane and applied them as proton exchange membranes in microbial fuel cells for water treatment.

However, the water solubility of the ILs can compromise the stability of the membrane due to their possible leaching out from the membrane structure, thus hindering the possible exploitation of ILs-based membranes on a larger scale. One possible solution can be represented by the use of polymerized ionic liquids, which can be obtained through the polymerization of ILs bearing suitable polymerizable groups. However, to the best of our knowledge, just a few works are currently available in the literature reporting the use of polymerized ionic liquids for the production of conductive membranes for electrochemical processes [21–24].

In particular, while imidazolium-based polymerizable ILs (PILs) have been alreadyexplored as monomers for the production of membranes for various applications, including some recent challenging applications in water decontamination [25], phosphonium-based analogues PILs have received much less attention even though the corresponding membranes may exhibit comparable ion conductivity, higher chemical stability, and wider electrochemical operating window [26–28].

In this work, we have carried out, for the first time, a systematic study on the use of a series of phosphonium-based PILs for the production of anion-conducting membranes. The main idea of this research was the possibility of properly balancing the low resistance transport of anions among cages composed of cationic branch chains, with a good stability in alkaline medium, tailoring the chemistry and microstructure of these materials. With this aim, phosphonium-based PILs were selected in the form of trialkylphosphonium salts with various alkyl chain lengths and different anionic counterparts. The selected PILs were photopolymerized, exploiting the reactivity between acrylate and styrene groups, using a special patented acrylate-based formulation [12,29] in order to produce stable and flexible membranes, avoiding any possible release from the polymer matrix. The results obtained highlighted a relevant effect of chain length and anionic counterion on the membrane's electrochemical properties and stability, demonstrating the possibility to tailor membrane electrochemical properties and microstructure by working on the chemical nature of the starting PIL.

2. Materials and methods

2.1. PIL synthesis

Polymerizable ionic liquids were synthesized as previously reported [12]. Briefly, PILs were synthesized by a two-step procedure based on quaternization of the trialkyl phosphine with 4-vinylbenzyl chloride to afford the corresponding phosphonium chloride, followed by anionic exchange. The chemical structure of the PIL used for membrane preparation is reported in Table 1.

2.2. Membrane preparation

2-Hydroxyethyl methacrylate (HEMA), ethylene glycol dimethacrylate (EGDMA), dodecyltrimethyl ammonium bromide (DTAB), 2,2-dimethoxy-2-phenylacetophenone (DMPA), sodium chloride (NaCl) and sodium hydroxide (NaOH) were purchased from Sigma-Aldrich (now Merck) and used without further purification.

The PIL-based membranes were prepared by solution casting and photopolymerization procedure [12]. HEMA (52 wt %) was mixed with water (8 wt %), DTAB (13 wt %), and the selected PIL (27 wt %). EGDMA (3 wt % on the weight of HEMA + PIL) and DMPA (0.6 wt % on the weight of the total solution) were finally added to the mixture and stirred for 1h. The homogenous solution was then poured between two glass plates kept at a distance of 100 μm by a spacer in order to fix the initial thickness of the liquid film which is then photo-polymerized for 3 min under UV light (Zp lamp emission from 180 nm to visible light, Helios Italquarz s.r.l.). The polymerized membranes were soaked in water in order to detach them from the glass plates and stored in water until their use. The PILs used for the preparation of the membranes and the related membrane identification codes are shown in Table 1. A similar procedure was used for the preparation of the blend membranes (Table 2).

Table 1
PILs used for membrane preparation and related membrane codes.

Chemical structure of the cationic part of the PIL	Anionic part the PIL	PIL code	PIL molecular weight (g mol^{-1})	Membrane code
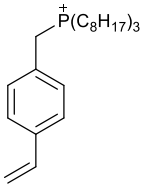	Tf_2N^-	PIL-Ph1	768	MPIL-Ph1
	PF_6^-	PIL-Ph2	633	MPIL-Ph2
	BF_4^-	PIL-Ph3	575	MPIL-Ph3
	Cl^-	PIL-Ph4	523	MPIL-Ph4
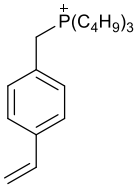	BF_4^-	PIL-Ph5	406	MPIL-Ph5
	Cl^-	PIL-Ph6	355	MPIL-Ph6
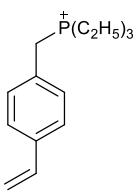	BF_4^-	PIL-Ph7	322	MPIL-Ph7
	Cl^-	PIL-Ph8	271	MPIL-Ph8

Table 2
PILs used in the blend membranes and related membrane codes.

PIL-Ph4 (wt %)	PIL-Ph8 (wt %)	Membrane code
75	25	MPIL-Ph9
50	50	MPIL-Ph10

2.3. Membrane characterization

Scanning Electron Microscopy (SEM) images of the prepared membranes were analysed by using a Zeiss, EVO MA10 microscope. Membrane samples were previously sputter-coated with a thin layer of gold (sputter machine Quorum Q 150R S) before SEM analyses.

Water uptake measurements were performed by weighing three different membrane samples before and after immersion in water for 48 h. The water uptake was then calculated using the following formula:

$$\text{Water uptake } (\%) = \frac{W_{w-}\ W_d}{W_d}\ x\ 100$$

where W_w and W_d are the weights of the membranes in wet and dry states, respectively.

Electrochemical impedance spectroscopy (EIS) experiments were carried out with a potentiostat/galvanostat combined with a frequency response analyzer (Metrohm Autolab PGSTAT302N) in the frequency range 100000-1 Hz, with a signal amplitude of 10 mV. A four-electrode configuration was used for the through-plane test in NaCl solution using an impedance cell having an active membrane area of 3.14 cm^2 [30]. The cell was fed by two gear pumps with two identical solutions (NaCl 0.5 mol/L at 25±3°C), kept under stirring and flowing along the opposite sides of the membrane (1.5 cm s^{-1}). The cell was placed inside a thermostatic Faraday cage for shielding purposes. Blank experiments were carried out without the membrane to determine the solution resistance. The membrane and solution resistance impedance spectra were fitted by the software Nova 1.9.16 by Metrohm Autolab B.V. in order to determine the membrane resistance as previously reported [31]. The membrane ionic conductivity was calculated from the membrane ionic resistance as follows:

$$Conductivity\ \left(mS\ cm^{-1}\right) = \frac{Thickness\ (cm)}{Resistance\ (\Omega) * Active\ Area\ (cm^2)} * 1000$$

Before the EIS tests, the membrane samples were activated in an aqueous solution 0.5 mol/L NaCl changing the solution three times along 24 hours. This testing solution was selected in order to easily compare the performance of the produced membranes with literature data where the membrane conductivity is frequently measured in this reference solution. The activation procedure is necessary to ensure that the membrane reach the equilibrium water uptake and ion composition in the testing condition.

Membrane permselectivity [32] was calculated as the ratio of the measured potential across the membrane separating two solutions of different concentration (NaCl 0.1 and 0.5 mol/L at 25±3°C) and theoretical value (37.8 mV):

$$Permselctivity\ (\%) = \frac{\text{measured potential } (mV)}{theoric\ \text{potential (mV)}} * 100$$

The membrane potential was measured by two Ag/ AgCl reference electrodes (Gamry Instruments) and a digital multimeter (Fluke 289/ FVR/IR3000, Fluke Europe B.V.).

Before the permselectivity tests, the membrane samples were activated in a 0.5 mol/L NaCl solution in water changing the solution three times during 24 hours. For comparison purpose, EIS and permselectivity tests were also carried out on benchmark AEMs in the same experimental conditions: Fumasep FAS (Fumatech); Neosepta® AMX (Astom Corp.); AEM-80045 (Fujifilm).

Moreover, in order to asses the membrane stability in alkaline medium the PIL-based membranes were converted in OH^- form by immersion in a NaOH solution (0.5 M) for 1 hour at room temperature. Then the solution was replaced with fresh 0.5 M NaOH and soaked again for 1 h. After the two soaks, the membrane was rinsed with deionized water until neutrality. A further stability test consisted in the immersion of the sample in a NaOH solution 30wt % at 80°C for 24 h and then rinsed with deionized water until neutrality.

Mechanical properties of the membranes were measured in stress-strain elongation experiments using ZWICK/ROELL Z 2.5 instrument.

Small-Angle X-ray Scattering (SAXS) measurements were carried out with Anton Paar's SAXSpoint 5.0 SAXS instrument on membranes removed from water and dried at room temperature. The system was equipped with a Primux 100 microfocus X-ray source (Cu Kα radiation, λ = 0.154 nm) and an EIGER2 R 1M photon counting detector, which was also used to measure the transmittance of the sample and to obtain the intensities scattering on an absolute scale.

The scattered intensity as a function of **q** gives insights into the distribution and arrangement of nanostructures. The positions of the peaks in the SAXS pattern indicate characteristic distances between repeating structures within the sample. The relationship between peak position q and the real-space distance *d* is given by:

$$d = \frac{2\pi}{q}$$

Differential scanning calorimeter (NEXTA DSC200, Itachi High-Tech) was used to determine the glass transition temperature (Tg) of the membrane. The membrane was dried at room temperature for 24 h, then 5 mg of each sample were sealed in DSC aluminium pan and tested under inert nitrogen atmosphere (50 mL/min) while ramping the temperature from -20°C to 180°C at 10°C/min rate.

Subsequently the sample was subjected to a cooling cycle and finally to a second heating cycle, all of them in the same temperature range and with the same heating/cooling rate. The Tg was determined in the second heating run in order to eliminate any signal due to residual absorbed water still present in the first run which could cover other signals in the thermogram. In order to determinate the Tg, the DSC signal and its derivative (DDSC) were monitored. The DSC inflections were attributed to Tg if they correspond in the DDSC signal to a maximum point.

3. Results and discussion

Eight phosphonium based PILs in the form of trialkylphosphonium salts with the alkyl chain ranging from C2 (ethyl) to C8 (octyl) and different inorganic (Cl^-, BF_4^-, PF_6^-) or organic (bis(trifluoromethanesulfonyl)azanide Tf_2N^-) counter-ions, were mixed with an acrylate monomer (HEMA), a diacrylate crosslinker (EGDMA) and a photo-initiator (DMPA) to produce the membranes by casting and successive photopolymerization, almost solvent free (Table 1, Fig. 1,).

Only a small percentage of water and a surfactant (DTAB) were necessary in order to obtain a homogeneous pre-polymerization solution. The absence of organic solvents in a castable solution, associated with a photopolymerization process, renders the method for producing PIL-based membranes scalable and quite sustainable. Moreover, operating in pseudo-neat conditions, the control of the final membrane thickness was quite easy because it resulted close to the initial thickness of the liquid polymerization layer poured between the two glass plates (100±10 μm).

The membranes prepared with the first seven PILs (from MPIL-Ph1 to MPIL-Ph7, Table 1) were dense and flexible and completely stable after prolonged contact with aqueous and saline solutions (>>6 months). In Fig. 2, it is possible to observe the typical aspect and dense morphology of a PIL-based membrane and its dense structure.

The crosslinking reaction avoided the dissolution of the polymer matrix in water, which represents the main limitation in the use of standard ionic liquids as membrane material for applications in aqueous solution.

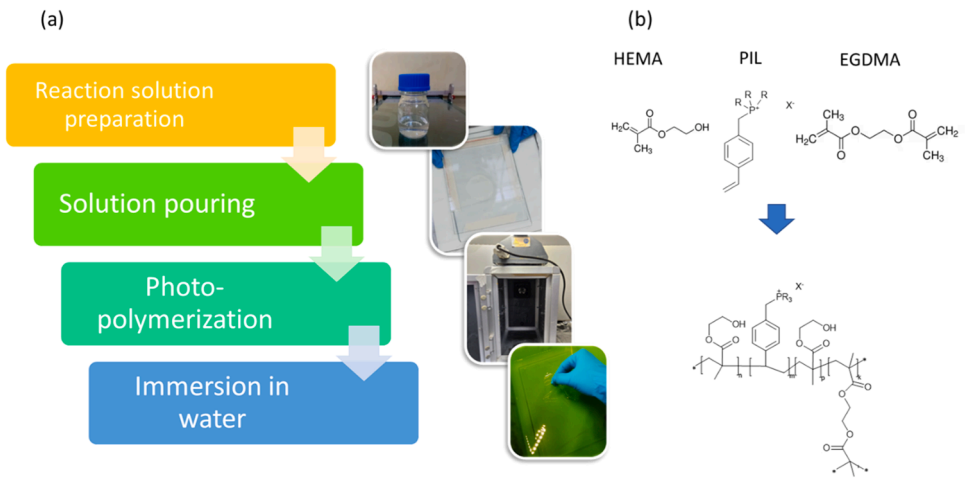

Fig. 1. Schematic illustration of the membrane fabrication procedure (a) and chemical formula of polymerized ionic liquid repeating unit formed by the reaction between HEMA, PIL and EGDMA (b).

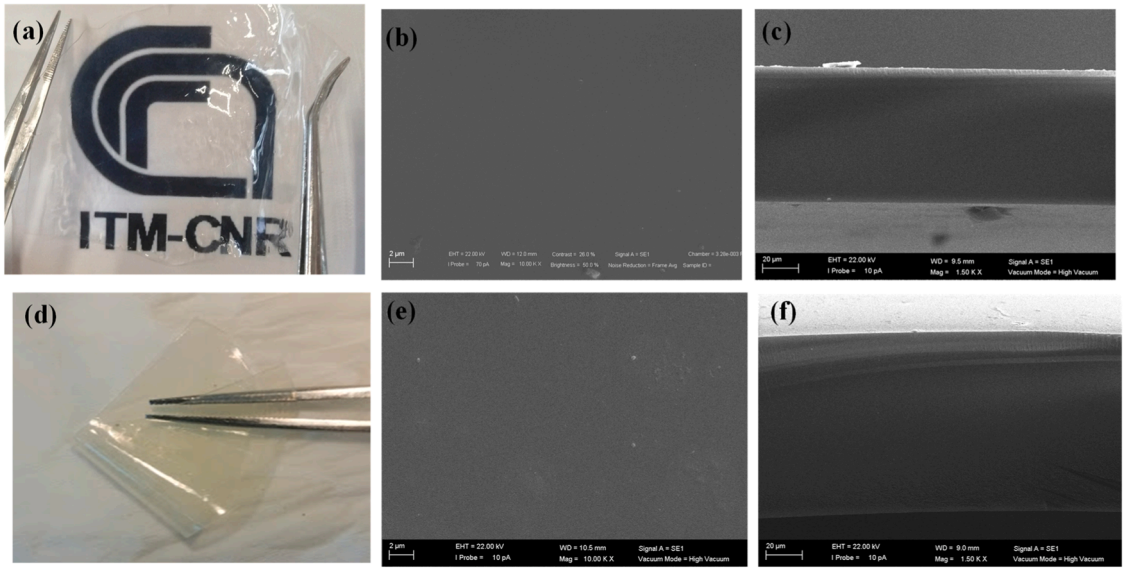

Fig. 2. Picture (a) and SEM images of the surface (b) and cross section (c) of the MPIL-Ph-3 membrane as prepared, and after stability test in concentrated NaOH (30wt % at 80°C for 24 h): picture (d), SEM images of the surface (e) and cross section (f).

The mechanical properties of the membranes in humidified state were good with the only exception of the MPIL-Ph8 which showed a limited stability in water because of the high hydrophilic character due to the combination of short alkyl groups (C2) with a small inorganic counter ion (Cl^-), causing an excessive water uptake (>100 %) and membrane softening.

Excluding MPIL-Ph8, the other PIL-based membranes resulted also mechanically stable after ion exchange procedure to place them in OH^-form. Moreover, on the membrane MPIL-Ph3 a stability test was carried out immersing the membrane in NaOH 30wt % at 80°C for 24h. The membranes resulted still flexible and despite a moderate change in colour (Fig. 2d), no fractures (Fig. 2 e-f) or appreciable change in weight were registered.

Both elastic behaviour of the PIL-based membranes is affected by their water content. In fact, MPIL-Ph3 membrane was stiffer with respect MPIL-Ph5 (same counterion ion but longer alkyl group, Table 1) because of the lower water uptake (Table 3).

Although the poor mechanical properties of the MPIL-Ph8, the interesting conductivity of this membrane (Cl^- conductivity: 8,74±0,04 mS/cm at 25±3°C), motivated further investigation in the form of blend membranes in combination with the less hydrophilic (but also less conductive) MPIL-Ph4 (Cl^- conductivity: 0,072±0,003 mS/cm at 25 ±3°C). The scope of the blending strategy was to assess the possibility to combine PILs with different properties to obtain membranes with tailored properties exploiting the specific advantages of each component. The prepared blend membranes (Table 2) were completely dense, homogenous, and stable in water. Their conductivity depended on the relative percentage of the two PILs used for preparing them and increased as the MPIL-Ph8 percentage grew larger (Cl^- conductivity: 0,2262±0,001 and 1,74±0,01 mS/cm at 25±3°C, for the blend membranes MPIL-Ph9 and MPIL-Ph10, respectively). Even though, the performances of the two blend membranes don't overcome in relevant way

Table 3
Water uptake and mechanical properties of PIL-based membranes.

Membrane	Water uptake (%)	Elastic modulus (MPa)	Elongation at break (%)
MPIL-Ph3	9±1	21 ± 2	42± 2
MPIL-Ph5	27±2	13 ± 2	46 ± 8

those of other single PIL membranes investigated, the proof of the concept of the blending strategy was validated demonstrating the possibility to expand the effective portfolio of properties of the PIL-based membrane materials.

Electrochemical impedance spectroscopy combined with membrane potential measurements pointed out a trade-off relationship between the ionic conductivity and permselectivity of the PIL-based membranes (Fig. 3).

The value of conductivity was influenced by both, the side chain length and the size of the counterion, with the effect of the first parameter more relevant than the second one. Increasing the length of the alkyl groups linked to phosphorus, the membrane conductivity was reduced. Moreover, the chemical nature of the counterion plays a similar effect, with the conductivity being favoured by smaller couterions (ionic radius: $Cl^- < BF_4^- < PF_6^- < Tf_2N^-$). The opposite trend was observed for the membrane permselectivity, favoured by longer side chain length and larger counterion. However, membranes combining long chains with a large anion paid an additional price in terms of permselectivity because of the higher electrochemical shielding of the cationic groups resulted in less permselective membranes (MPIL-Ph1 and MPIL-Ph2 vs MPIL-Ph3). The same tests were carried out with benchmark anion exchange membranes: Fumasep FAS (Fumatech); Neosepta® AMX (Astom Corp.); AEM-80045 and (Fujifilm). Whereas for Selemion AMN (Ashai Glass), the producer's specifications were used [33] (Fig. 3). Although some of the commercial membranes resulted in higher performance in sodium chloride solution than the PIL-based membranes, the possibility of achieving tuneable conductivity and permselectivity by a rational design of the PIL used for preparing the membrane, or blending different materials, represented a further step toward the development next generation membranes for energy.

The experimental results obtained are consistent with an effect of alkyl chain length and size of the counter ion on membrane microstructure in terms of dimensions, tortuosity, and interconnection of the hydrophilic channels, which influence the membrane transport properties. For large counterions, such as Tf_2N^- and PF_6^-, loose ionic aggregates are formed leading to a low interconnection of the hydrophilic channels. This observation is consistent with the appearance of scattering peaks at lower values of the transferred momentum q (i.e., corresponding to larger characteristic distances) in the SAXS spectra. Fig. 4a.1 and 4a.2 show display the two-dimensional SAXS patterns of samples MPIL-Ph1 and MPIL-Ph2, respectively. As can be seen, in addition to the scattering at low angles around the beam-stopper (pin

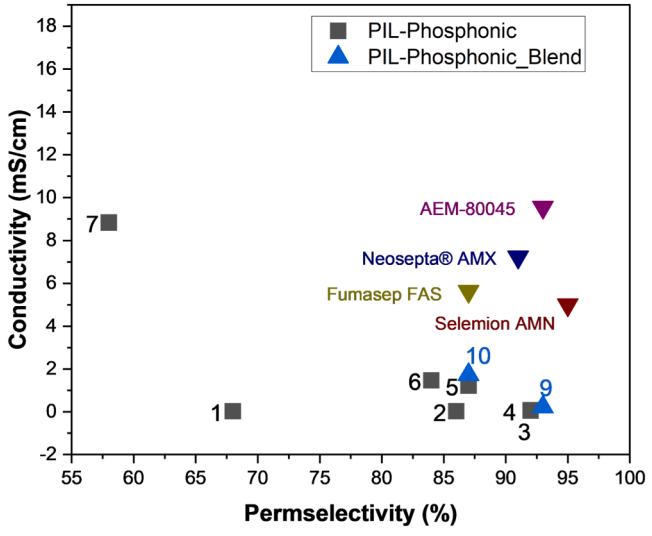

Fig. 3. Conductivity vs permselectivity of the PIL-based membranes (for sake of clarity, only the number of each membrane code of Table 1 and Table 2 is reported in the graph) and commercial membranes.

whose tip is located at $q_x=q_y=0$), a circular bright region appears at values of q around 1 nm^{-1}. This is further emphasized in Fig. 4b.1 and 4b.2, where it is shown the integration of the 2D spectrum over $0< \varphi<180°$. The presence of a peak at 0.89 and 1.04 nm^{-1} is, indeed, evident for MPIL-Ph1 and MPIL-Ph2, respectively (see red dashed line in Fig. 4b.1 and 4b.2).

The vertical red dashed line in (b.1, b.2) marks the position of the main scattering peak. The curves (c.1, c.2) represent for MPIL-Ph1 and MPIL-Ph2, respectively, the averaged intensity distribution calculated around the peak position, while the horizontal red dashed line indicates the mean intensity value within the selected q-range.

Panels (d-j) show the SAXS spectra of samples MPIL-Ph1 through MPIL-Ph7. The vertical dashed lines highlight the position of the peak corresponding to the lowest scattering vector (q).

Another relevant feature in the 2D patterns of Fig. 4a.1 and 4a.2 is the isotropic nature of the scattering. This isotropy is confirmed by the azimuthal intensity plots in Fig. 4c.1 and 4c.2, obtained by integrating the 2D signal over q values between 0.5 and 1.5 nm^{-1}, i.e., around the main peak. The intensity oscillates around a nearly constant average value (indicated by the red dashed horizontal line in Fig. 4c.1 and 4c.2) with a noise-like profile, which is characteristic of isotropic structures. This isotropy is observed not only for MPIL-Ph1 and MPIL-Ph2, but across all investigated membranes. For the sake of completeness, Fig. 4d-j reports the 1D SAXS spectra of all samples vs. q. In order to provide the fairest comparison, all spectra were acquired under the same experimental conditions, namely, with the same sample-to-detector distance corresponding to a maximum value of transferred momentum of 6 nm^{-1}. The panels of Fig. 4d-j were sorted also following the samples' conductivity. As can be seen, all the spectra show a peak, indicated by vertical dashed lines, except that of MPIL-Ph7. In this regard, however, it should be noted that the intensity of the peak decreases with its spectral position, that is, peaks located at higher values of q have a lower intensity. For this reason, it is reasonable to assume that MPIL-Ph7 may have a peak at a higher value of q, which is either above our spectral range (i.e., above 6 nm^{-1}) or with such a low intensity that is not detectable with our device within a reasonably short acquisition time. Such a hypothesis is further confirmed by the monotonic trend of the peak position vs. the sample conductivity (Fig. 5a).

Conductivity dependence on the characteristic distance between repeating structures attributed to the ionic clusters within the membrane (Fig. 5a), allows to conceptually subdivide the PIL-based membranes in three groups: long chain and large anion (MPIL-Ph1 and MPIL-Ph2); long chain and small anion (MPIL-Ph3 and MPIL-Ph4); medium chain and small anion (MPIL-Ph5 and MPIL-Ph6).

The same trend was observed in terms of the dependence of conductivity on the mean free path (MFP) and free volume (FV) estimated by ^{129}Xe NMR experiments in a previous work [12] on some of the samples investigated in this work. The conductivity decreases with the increasing values of characteristic distance, MFP, and FV. In other words, the membrane conductivity was strictly related to the membrane's microstructure, which, in turn, depends on the chemical structure and hydrophilicity of the PIL-based polymer matrix. It is worth noting that other authors [34] reported that increasing the chain length of substituent groups of the PILs leads to an increased ionic conductivity under anhydrous conditions in the corresponding PIL-based membrane due to a reduction in glass transition with consequent higher polymer segmental motion, as explained in the Vogel-Tammann-Fulcherb (VTF) model [35,36]. In polymer electrolytes, lower Tg generally increases ionic conductivity because it means more polymer segmental motion, creating pathways for ions to move and reducing the mass transport resistance. Moreover, water molecules generally act as plasticizer in polymers, significantly decreasing Tg by inserting themselves between polymer chains and increasing free volume and facilitating chain movement through hydrogen bonding, making the polymer more soft and flexible. The effect is more relevant in hydrophilic polymers where water interacts with polar groups forming hydrogen bonds (bound

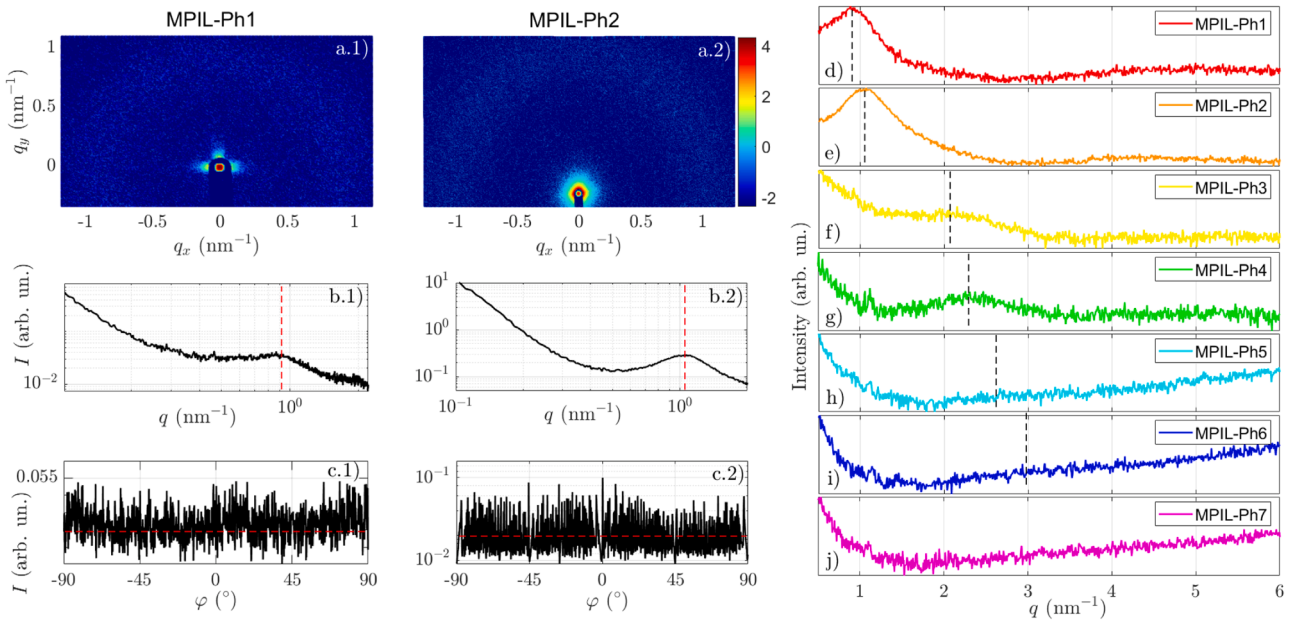

Fig. 4. SAXS spectra of PIL-based membranes: (a.1) and (a.2) are the two-dimensional SAXS patterns of samples MPIL-Ph1 and MPIL-Ph2, respectively; (b.1, b.2) and (c.1, c.2) present the corresponding one-dimensional SAXS profiles obtained integration of the 2D patterns over φ or q.

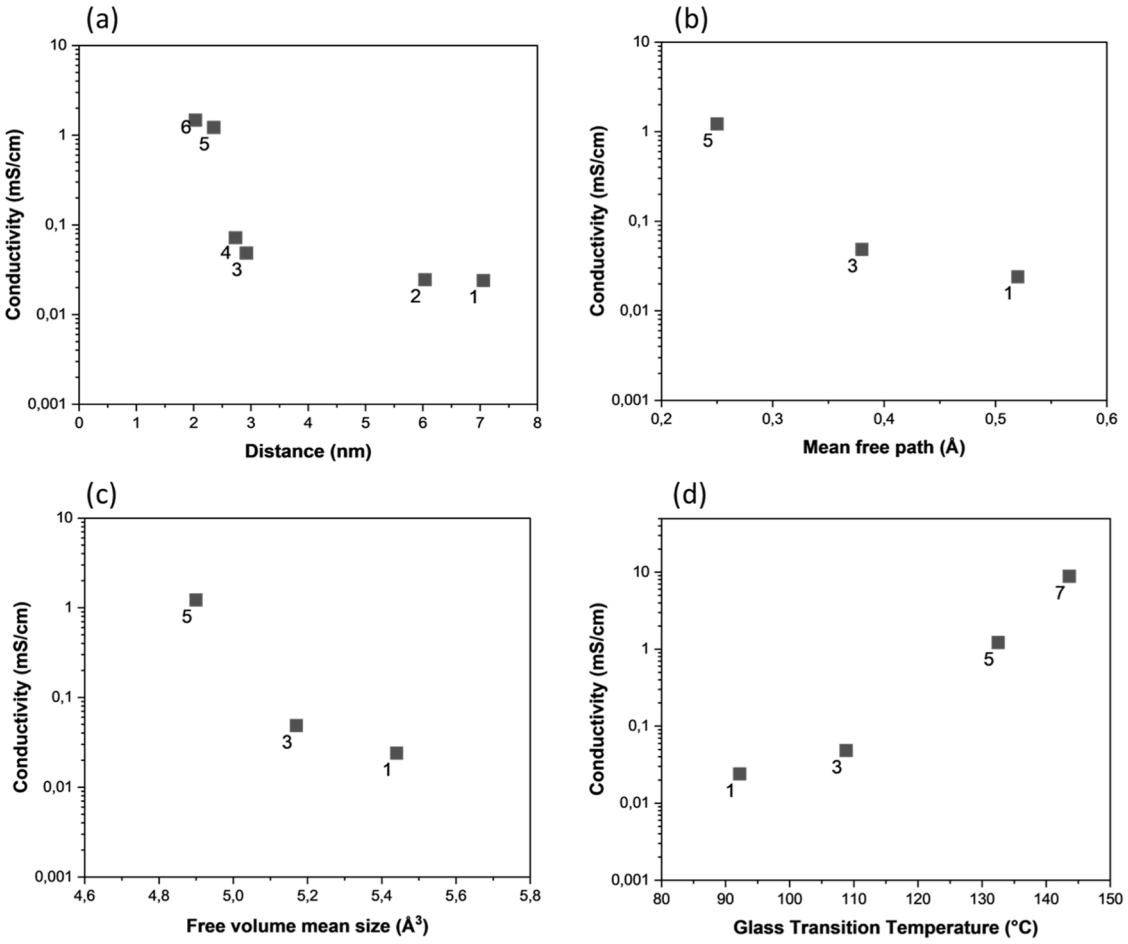

Fig. 5. Conductivity (Cl^- at at 25±3°C) dependence from: (a) characteristic distance calculated from SAXS peak position , (b) mean free path (MFP) and (c) free volume (FV) mean size from ^{129}Xe NMR and (c) glass transition temperature of the membrane from DSC. MFP and FV data from [12].

water, non-freezable). However, water that exists in clusters or in a more bulk-like state (free water, freezable) contributing less to plasticization

than bound water [37] but playing a crucial role in water-assisted ion transport. Depending on the water absorption level, anion transport in conducting membranes is governed by three main transport mechanisms: surface site hopping, vehicular transport, and Grotthuss hopping (only for OH^- ion) [38]. At low hydration levels, the hopping of anions between solvation sites is the main anion transport mechanism, and it is strongly influenced by the segmental mobility and solvation environment of the polymer chain. However, when the membrane is in a high humidification state, the predominant mechanism of conduction is the vehicular and, only for OH^- transport, the Grotthuss mechanisms, due to ionic motion through the hydrophilic channel formed by the ionic cluster and bulk water.

Increasing the alkyl chain length of the PIL, the glass transition temperature of the corresponding membranes decreases but also the ionic conductivity declines (from C2 to C4 and C8 with BF_4^- as counterion, for MPIL-Ph7, MPIL-Ph5 and MPIL-Ph3, respectively; Fig. 5d). Furthermore, increasing the count-ion size but maintaining the same alkyl group, the Tg is reduced and the conductivity, as well (C8 as alkyl group and counter ion BF_4^- for MPIL-Ph3 and Tf_2N^- for MPIL-Ph1; Fig. 5d). These results are in line with the overall anion transport mechanism in PIL-based membranes immersed in NaCl solution which is governed by a vehicular mechanism which involves concentration gradient-driven Cl^- diffusion and electromigration, strongly dependent from hydration level but not influenced in relevant way by polymer segmental motion.

Adapting the cluster network model [39] originally proposed to rationalize the transport mechanism in perfluorosulfonic acid membranes (e.g. Nafion), hydrophilic pockets whose size is in the order of a few nanometers are formed by the phosphonic ion exchange groups. In the presence of water, the polymer matrix hydration degree depends from the difference in hydrophilicity of the various component forming the polymer network. As a consequence, the dimensions of these clusters increase owing to the formation of hydrogen bonds with the absorbed free water, and the hydrophilic pockets are better interconnected by a network of channels separated from the hydrophobic region formed by the backbone of the polymer. The interconnection of the ion exchange phosphonium groups by hydrophilic channels increases with the increasing number of ion exchange groups per mass of polymer, as confirmed by plotting conductivity versus equivalent weight (i.e., the mass of polymer which contains one equivalent of ion exchange group) and, consequently, increases also with the water uptake (Fig. 6a-b).

Also, a recent molecular dynamics simulation study on PIL-based membranes confirms by quantitative analyses, including pore connectivity descriptors, ion-ion association free energies from radial distribution function integration, and backbone-water interaction profiles, that steric hindrance of the alkyl groups of phosphonium-type PILs modulates hydration shell formation, ion pairing, and channel percolation40].

4. Conclusions

Phosphonium-based polymerizable ionic liquids are versatile membrane materials that may undergo wide chemical variations in order to tailor the membrane's properties. Dense and completely stable membranes were prepared by a casting and photopolymerization process, under almost solvent-free conditions. The absence of organic solvents to have a castable solution, combined with a photopolymerization process renders the method to produce the PIL-based membranes scalable and quite sustainable. The membranes' properties were tuned by tailoring the chemical nature of the PIL used for preparing the membrane or blending PILs with different properties. A clear structure-property relationship was rationalized by chemical-physical and structural characterization techniques. Conductivity was higher for PIL-based membranes with shorter alkyl chain length (C2>C4>C6>C8) and smaller counterions (Cl^->BF_4^-> PF_6^- > Tf_2N^-). Our results pointed out a trade-off relationship between ionic conductivity and permselectivity, and are consistent with an effect of alkyl chain length and size of the counter ion on membrane microstructure and, as a consequence, on water uptake and ion transport. The main outcome of this research lies in the possibility to balance the low ionic resistance transport through the charged moieties with a good stability in aqueous medium, tailoring the chemistry of these materials. The obtained results encourage the use of PILs as engineered materials in tackling challenges in membranes for energy

Funding

This work has received funding from the European Union - Next Generation EU in the framework of the project PNRR - AdP IDROGENO (PRR.AP015.017.002; L.A. 1.1.6).

CRediT authorship contribution statement

Enrica Fontananova: Writing – review & editing, Writing – original draft, Validation, Supervision, Methodology, Investigation, Funding acquisition, Formal analysis, Data curation, Conceptualization. **Francesco Galiano:** Writing – review & editing, Writing – original draft, Investigation, Formal analysis, Data curation, Conceptualization. **Raffaella Mancuso:** Methodology, Investigation, Formal analysis, Data curation. **Daria Talarico:** Methodology, Investigation, Formal analysis. **Gianluca Di Profio:** Writing – review & editing, Writing – original draft, Methodology, Formal analysis, Data curation, Conceptualization.

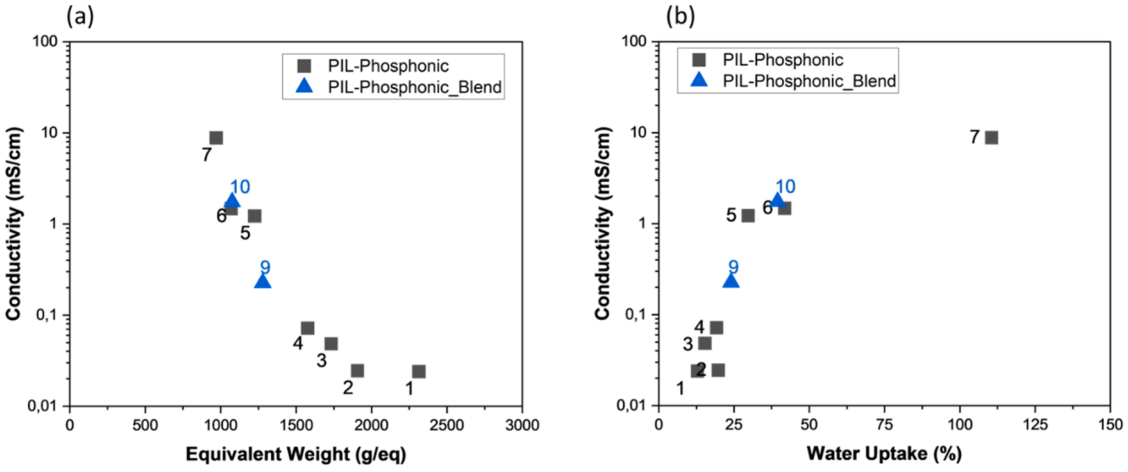

Fig. 6. Conductivity (Cl^- at at 25±3°C) vs (a) equivalent weight ad (b) water uptake.

Lorenzo Guazzelli: Methodology, Investigation, Formal analysis, Data curation. **Christian S. Pomelli:** Investigation, Formal analysis, Data curation. **Mario Ferraro:** Writing – review & editing, Writing – original draft, Methodology, Formal analysis, Data curation. **Raffaele Filosa:** Methodology, Investigation, Formal analysis, Data curation. **Vincenzo Formoso:** Methodology, Formal analysis, Data curation. **Raffaele G. Agostino:** Methodology, Formal analysis, Data curation. **Bartolo Gabriele:** Writing – review & editing, Writing – original draft, Supervision, Data curation, Conceptualization. **Alberto Figoli:** Writing – review & editing, Writing – original draft, Supervision, Funding acquisition, Conceptualization.

Declaration of competing interest

The authors declare that they have no known competing financial interests or personal relationships that could have appeared to influence the work reported in this paper.

Acknowledgments

This work has received funding from the European Union - Next Generation EU in the framework of the project PNRR - AdP IDROGENO (PRR.AP015.017.002; L.A. 1.1.6). Prof. Fiore Nicoletta (University of Calabria, Italy) is gratefully acknowledged for DSC measurements.

Data availability

Data will be made available on request.

References

[1] N.P. Berezina, N.A. Kononenko, O.A. Dyomina, N.P. Gnusin, Characterization of ion-exchange membrane materials: Properties vs structure, Adv. Colloid Interface Sci. 139 (2008) 3–28, https://doi.org/10.1016/j.cis.2008.01.002.
[2] S. Jiang, H. Sun, H. Wang, B.P. Ladewig, Z. Yao, A comprehensive review on the synthesis and applications of ion exchange membranes, Chemosphere 282 (2021) 130817, https://doi.org/10.1016/j.chemosphere.2021.130817.
[3] P. Zuo, Z. Xu, Q. Zhu, J. Ran, L. Ge, X. Ge, L. Wu, Z. Yang, T. Xu, Ion Exchange Membranes: Constructing and Tuning Ion Transport Channels, Adv. Funct. Mater 32 (2022) 2207366, https://doi.org/10.1002/adfm.202207366.
[4] M.A. Hickner, A.M. Herring, E.B. Coughlin, Anion exchange membranes: Current status and moving forward, J. Polym. Sci. Part B Polym. Phys. 51 (2013) 1727–1735, https://doi.org/10.1002/polb.23395.
[5] C. Cheng, Z. Yang, J. Pan, B. Tong, T. Xu, Facile and cost effective PVA based hybrid membrane fabrication for acid recovery, Sep. Purif. Technol. 136 (2014) 250–257, https://doi.org/10.1016/j.seppur.2014.09.013.
[6] Y. He, J. Pan, L. Wu, L. Ge, T. Xu, Facile preparation of 1,8-Diazabicyclo [5.4.0] undec-7-ene based high performance anion exchange membranes for diffusion dialysis applications, J. Memb. Sci. 491 (2015) 45–52, https://doi.org/10.1016/j.memsci.2015.04.055.
[7] X. Yue, W. Wu, G. Chen, C. Yang, S. Liao, X. Li, Influence of 2,2′,6,6′-tetramethyl biphenol-based anion-exchange membranes on the diffusion dialysis of hydrochloride acid, J. Appl. Polym. Sci. 134 (2017) 45333, https://doi.org/10.1002/app.45333.
[8] K. Emmanuel, C. Cheng, B. Erigene, A.N. Mondal, N.U. Afsar, M.I. Khan, M. M. Hossain, C. Jiang, L. Ge, L. Wu, T. Xu, Novel synthetic route to prepare doubly quaternized anion exchange membranes for diffusion dialysis application, Sep. Purif. Technol. 189 (2017) 204–212, https://doi.org/10.1016/j.seppur.2017.08.005.
[9] K. Emmanuel, C. Cheng, B. Erigene, A.N. Mondal, M.M. Hossain, M.I. Khan, N. U. Afsar, G. Liang, L. Wu, T. Xu, Imidazolium functionalized anion exchange membrane blended with PVA for acid recovery via diffusion dialysis process, J. Memb. Sci. 497 (2016) 209–215, https://doi.org/10.1016/j.memsci.2015.09.043.
[10] K. Emmanuel, B. Erigene, C. Cheng, A.N. Mondal, M.M. Hossain, M.I. Khan, N. U. Afsar, L. Ge, L. Wu, T. Xu, Facile synthesis of pyridinium functionalized anion exchange membranes for diffusion dialysis application, Sep. Purif. Technol. 167 (2016) 108–116, https://doi.org/10.1016/j.seppur.2016.05.006.
[11] E. Fontananova, D. Messana, R.A. Tufa, I. Nicotera, V. Kosma, E. Curcio, W. van Baak, E. Drioli, G. Di Profio, Effect of solution concentration and composition on the electrochemical properties of ion exchange membranes for energy conversion, J. Power Sources. 340 (2017) 282–293, https://doi.org/10.1016/j.jpowsour.2016.11.075.
[12] F. Galiano, R. Mancuso, L. Guazzelli, M. Mauri, C. Chiappe, R. Simonutti, A. Brunetti, C.S. Pomelli, G. Barbieri, B. Gabriele, A. Figoli, Phosphonium ionic liquid-polyacrylate copolymer membranes for improved CO2 separations, J. Memb. Sci. 635 (2021) 119479, https://doi.org/10.1016/j.memsci.2021.119479.
[13] M. Zhang, L. Chen, Z. Yuan, R. Semiat, X. He, CO_2-Philic Imidazolium-Based Poly (Ionic Liquid) Composite Membranes for Enhanced CO_2/N_2 Separation, Ind. Eng. Chem. Res. 62 (2023) 8902–8910, https://doi.org/10.1021/acs.iecr.3c01083.
[14] S. Ravula, K.W. Wise, P.S. Shinde, J.E. Bara, Design and Performance of Di- and Tricationic Poly(ionic liquid) + Ionic Liquid Composite Membranes for CO2 Separation, Macromolecules 56 (2023) 6126–6141, https://doi.org/10.1021/acs.macromol.3c00850.
[15] L.P. Silva Eyad Qasem, L. Upadhyaya, R. Esposito, R. Górecki, J.A.P. Coutinho, P. J. Carvalho, S.P. Nunes, Encapsulated Amino Acid-Based Ionic Liquid for CO_2 Separation Membranes ACS Sustainable Chem, Eng 12 (2024) 300–309, https://doi.org/10.1021/acssuschemeng.3c05135.
[16] N.S. Naik, M. Padaki, S. Déon, D.H.K. Murthy, Novel poly (ionic liquid)-based anion exchange membranes for efficient and rapid acid recovery from industrial waste, Chem. Eng. J. 401 (2020) 126148, https://doi.org/10.1016/j.cej.2020.126148.
[17] M. Guo, J. Fang, H. Xu, W. Li, X. Lu, C. Lan, K. Li, Synthesis and characterization of novel anion exchange membranes based on imidazolium-type ionic liquid for alkaline fuel cells, J. Memb. Sci. 362 (2010) 97–104, https://doi.org/10.1016/j.memsci.2010.06.026.
[18] C.Y. Wong, W.Y. Wong, K.S. Loh, K.L. Lim, Protic ionic liquids as next-generation proton exchange membrane materials: Current status & future perspectives, React. Funct. Polym. 171 (2022) 105160, https://doi.org/10.1016/j.reactfunctpolym.2022.105160.
[19] N.A.H. Rosli, K.S. Loh, W.Y. Wong, R.M. Yunus, T.K. Lee, A. Ahmad, S.T. Chong, Review of Chitosan-Based Polymers as Proton Exchange Membranes and Roles of Chitosan-Supported Ionic Liquids, Int. J. Mol. Sci. 21 (2020) 632, https://doi.org/10.3390/ijms21020632.
[20] F.J. Hernández-Fernández, A. Pérez de los Ríos, F. Mateo-Ramírez, C. Godínez, L. J. Lozano-Blanco, J.I. Moreno, F. Tomás-Alonso, New application of supported ionic liquids membranes as proton exchange membranes in microbial fuel cell for waste water treatment, Chem. Eng. J. 279 (2015) 115–119, https://doi.org/10.1016/j.cej.2015.04.036.
[21] J. Fang, M. Lyu, X. Wang, Y. Wu, J. Zhao, Synthesis and performance of novel anion exchange membranes based on imidazolium ionic liquids for alkaline fuel cell applications, J. Power Sources. 284 (2015) 517–523, https://doi.org/10.1016/j.jpowsour.2015.03.065.
[22] G. Huang, L. Porcarelli, Y. Liang, M. Forsyth, H. Zhu, Influence of Counteranion on the Properties of Polymerized Ionic Liquids/Ionic Liquids Proton-Exchange Membranes, ACS Appl. Energy Mater. 4 (2021) 10593–10602, https://doi.org/10.1021/acsaem.1c01571.
[23] T.T. Zuo, K. Liu, X.Q. Wei, S. Hu, Q.T. Che, Constructing lamellar low temperature anion exchange membranes based on polymerized ionic liquid and graphene oxide nanosheets, Mater. Today Chem. 31 (2023) 101615, https://doi.org/10.1016/j.mtchem.2023.101615.
[24] E. Fontananova, R. Ciriminna, D. Talarico, F. Galiano, A. Figoli, G. Di Profio, R. Mancuso, B. Gabriele, C.S. Pomelli, L. Guazzelli, G. Angellotti, G. Li Petri, F. Meneguzzo, M. Pagliaro, CytroCell@PIL: A New Citrus Nanocellulose-Polymeric Ionic Liquid Composite for Enhanced Anion Exchange Membranes, Nano Select 0 e70001 (2025) 1–8, https://doi.org/10.1002/nano.70001.
[25] F. Galiano, R. Mancuso, L. Guazzelli, C.S. Pomelli, J. Bundschuh, J. Rinklebe, S.-L. Wang, C. Apollaro, F. Palumbo, C. Chiappe, A. Figoli, B. Gabriele, Arsenic water decontamination by a bioinspired As-sequestering porous membrane, Nature Water 2 (4) (2024) 350–359, https://doi.org/10.1038/s44221-024-00220-x.
[26] M. Chen, B.T. White, C.R. Kasprzak, T.E. Long, Advances in phosphonium-based ionic liquids and poly(ionic liquid)s as conductive materials, Eur. Polym. J. 108 (2018) 28–37, https://doi.org/10.1016/j.eurpolymj.2018.08.015.
[27] C. Jangu, T.E. Long, Phosphonium cation-containing polymers: From ionic liquids to polyelectrolytes, Polymer 55 (2014) 3298–3304, https://doi.org/10.1016/j.polymer.2014.04.015.
[28] K.J. Fraser, D.R. MacFarlane, Phosphonium-Based Ionic Liquids: An Overview, Aust. J. Chem. 62 (2009) 309, https://doi.org/10.1071/CH08558.
[29] A. Figoli, F. Galiano, G. Barbieri, A. Brunetti, L. Giorno, C.S. Pomelli, C. Chiappe, B. Gabriele, R. Mancuso, Y. Itami, Membranes containing polymerised ionic liquid for use in gas separation, WO/2019/171409, 2019.
[30] E. Fontananova, W. Zhang, I. Nicotera, C. Simari, W. van Baak, G. Di Profio, E. Curcio, E. Drioli, Probing membrane and interface properties in concentrated electrolyte solutions, J. Memb. Sci. 459 (2014) 177–189, https://doi.org/10.1016/j.memsci.2014.01.057.
[31] E. Fontananova, D. Messana, R.A. Tufa, I. Nicotera, V. Kosma, E. Curcio, W. van Baak, E. Drioli, G. Di Profio, Effect of solution concentration and composition on the electrochemical properties of ion exchange membranes for energy conversion, J. Power Sources 340 (2017) 282–293, https://doi.org/10.1016/j.jpowsour.2016.11.075.
[32] G.M. Geise, M.A. Hickner, B.E. Logan, Ionic Resistance and Permselectivity Tradeoffs in Anion Exchange Membranes, ACS Appl. Mater. Interfaces 5 (20) (2013) 10294–10301, https://doi.org/10.1021/am403207w.
[33] https://www.agcchem.com (accessed on September 22nd, 2025).
[34] R. Löwe, T. Hanemann, T. Zinkevich, A. Hofmann, Structure-Property Relationship of Polymerized Ionic Liquids for Solid-State Electrolyte Membranes, Polymers 13 (5) (2021) 792, https://doi.org/10.3390/polym13050792.
[35] L.M Carvalho, P. Guégan, H. Cheradame, A.S Gomes, Variation of the mesh size of PEO-based networks filled with TFSILi: from an Arrhenius to WLF type conductivity behavior, Europ. Poly. J. 36 (2000) 401–409, https://doi.org/10.1016/S0014-3057(99)00057-9.

[36] S.B. Aziz, T.J. Woo, M.F.Z. Kadir, H.M. Ahmed, A conceptual review on polymer electrolytes and ion transport models, J. Sci. Advan. Mater. Devic. 3 (2018) 1–17, https://doi.org/10.1016/j.jsamd.2018.01.002.
[37] Y.J Yu, K. Hearon, T.S. Wilson, D.J. Maitland, The effect of moisture absorption on the physical properties of polyurethane shape memory polymer foams, Smart Mater. Struct. 20 (2011) 085010, https://doi.org/10.1088/0964-1726/20/8/085010.
[38] Z. Wang, G. Sun, N.H.C. Lewis, et al., Water-mediated ion transport in an anion exchange membrane, Nat Commun. 16 (2025) 1099, https://doi.org/10.1038/s41467-024-55621-z.
[39] K.A. Mauritz, R.B. Moore, State of Understanding of Nafion, Chem. Rev. 104 (2004) 4535–4585, https://doi.org/10.1021/cr0207123.
[40] J.H. Park, E. Fontananova, B. Gabriele, T.K. Lee, F. Galiano, C.H. Park, A. Figoli, E. Tocci, R. Mancuso, S.Y. Nam, From chain length to ion diffusion: Molecular insights into phosphonium-based polymerized ionic liquid membranes for energy applications, Desalination 617 (2026) 119434, https://doi.org/10.1016/j.desal.2025.119434.